Gastric Cancer (2014) 17:497–507
DOI 10.1007/s10120-013-0316-0

ORIGINAL ARTICLE

New whole-body multimodality imaging of gastric cancer peritoneal metastasis combining fluorescence imaging with ICG-labeled antibody and MRI in mice

Akihiro Ito · Yuichi Ito · Shigeru Matsushima · Daisuke Tsuchida · Mai Ogasawara · Junichi Hasegawa · Kazunari Misawa · Eisaku Kondo · Norio Kaneda · Hayao Nakanishi

Received: 26 August 2013 / Accepted: 4 November 2013 / Published online: 28 November 2013

Abstract
Background Peritoneal metastasis is the most frequent pattern of recurrence after curative surgery for gastric cancer. However, such a recurrence is difficult to detect by conventional computed tomography (CT) and magnetic resonance imaging (MRI) at an early stage. To improve the sensitivity and specificity of diagnostic imaging for peritoneal metastasis, we developed a new type of multimodality imaging combining fluorescence imaging with near-infrared fluorophore (NIR)-labeled antibodies and MRI.
Methods Dual optical imaging of peritoneal metastasis was carried out using luciferase-tagged gastric cancer cell lines and XenoLight CF750 or indocyanine green (ICG)-labeled anti-human epidermal growth factor receptor (EGFR) or CEA antibody as a probe in mice with Ivis in vivo imaging system.
Results This whole-body fluorescent imaging system sensitively detected metastatic foci <1 mm in diameter in the peritoneal cavity noninvasively. Fluorescence imaging proved to be specific because the fluorescence signal was abolished by blocking with excess unlabeled antibody. Although this fluorescence imaging had higher sensitivity for detection of small-sized peritoneal metastases than MRI, it proved difficult to accurately determine organ distribution of the metastasis. We thus developed a multimodality imaging system by the fusion of the three-dimensional fluorescence image with the MRI image and demonstrated its improved diagnostic accuracy over either method alone.
Conclusion The present results suggest that multimodality imaging consisting of fluorescence imaging with NIR-labeled EGFR or CEA antibody and MRI allows sensitive, specific, and anatomically accurate detection of peritoneal metastasis noninvasively at an early stage.

Keywords Molecular imaging · Fluorescence imaging · ICG · NIR-fluorophore · MRI · Multimodality imaging · Gastric cancer · Peritoneal metastasis · Cetuximab · CEA

Abbreviations

CT	Computed tomography
MRI	Magnetic resonance imaging
PET	Positron emission tomography
SPECT	Single photon emission computed tomography
EGFR	Epidermal growth factor receptor
NIR	Near-infrared
i.p.	Intraperitoneally
i.v.	Intravenously
3D	Three dimensional
ICG	Indocyanine green

A. Ito · E. Kondo · H. Nakanishi (✉)
Division of Oncological Pathology, Aichi Cancer Center Research Institute, Kanokoden, Chikusa-ku, Nagoya 464-8681, Japan
e-mail: hnakanis@aichi-cc.jp

A. Ito · D. Tsuchida · M. Ogasawara · N. Kaneda
Graduate School of Pharmaceutical Sciences, Meijo University, Nagoya, Japan

Y. Ito · K. Misawa
Department of Gastroenterological Surgery, Aichi Cancer Center Central Hospital, Nagoya, Japan

S. Matsushima
Department of Diagnostic and Interventional Radiology, Aichi Cancer Center Central Hospital, Nagoya, Japan

J. Hasegawa
Department of Mechanics and Information Technology, Chukyo University, Nagoya, Japan

Introduction

Although the survival of patients with gastric cancer has improved with the development of new diagnostic and therapeutic modalities, it remains one of the leading causes of cancer death in East Asian countries as well as in some Western countries. Peritoneal metastasis accounts for more than 50 % of the recurrence after curative surgery and is therefore the most life-threatening lesion in gastric cancer patients [1, 2]. Conventional whole-body imaging technologies such as computed tomography (CT) and magnetic resonance imaging (MRI) are powerful modalities for detecting metastases in solid organs such as liver, lung, bone, and lymph nodes and monitoring their recurrence. However, peritoneal metastases at an early stage consist of small flat lesions less than 1 cm in diameter on the surface of the peritoneal cavity, and they are difficult to diagnose by conventional CT/MRI [3]. Molecular imaging using labeled small-molecule tyrosine kinase inhibitors, peptides, and antibodies as molecular probes are potential alternatives for conventional image diagnostics [4], including positron emission tomography (PET), single photon emission computed tomography (SPECT), molecular MRI, and optical imaging [5, 6]. Among them, optical imaging modalities using bioluminescent- or fluorescent-labeled probes offer a technique with higher sensitivity and higher throughput imaging than PET/SPECT because of easy operation, short acquisition time, and lower cost [7]. Bioluminescent or fluorescent imaging using luciferase- or green fluorescent protein (GFP)-tagged cell lines is a widespread noninvasive, real-time in vivo imaging system, but this optical imaging requires gene transfection and therefore its use is limited to small animal models [8, 9]. Advantages of fluorescence imaging over luminescence imaging include the usability of a fluorophore-labeled probe instead of gene transfection and no need of a substrate for visualization. Major drawbacks of fluorescence imaging are low spatial resolution, limited depth of tissue penetration, and high background signal caused by autofluorescence from non-tumor tissues and ingested food [10]. The problem of poor anatomical imaging can be overcome by the use of MRI with the highest spatial resolution in combination with optical imaging [11]. In addition, limited depth penetration and high background signal can be partly overcome by the use of light in the near-infrared (NIR) range (700–900 nm), which is minimally absorbed by hemoglobin, muscle, and fat tissues, and minimizes autofluorescence of tissues [12]. Therefore, the NIR-fluorophore allows deeper tissue penetration of photons, which results in its potential application to noninvasive whole-body imaging for metastasis, especially peritoneal metastasis. For these reasons, this new multimodality imaging with combination of fluorescence imaging and MRI is a potential alternative for conventional CT/MRI for early diagnosis of peritoneal metastasis.

For optical imaging, selection of targeting molecules is critical for sensitive, specific, and safe detection of peritoneal metastasis [13]. A potential targeting molecule is epidermal growth factor receptor (EGFR), which is known to be frequently overexpressed and involved in the peritoneal metastasis of gastric cancers [14–16]. A chimeric human-murine EGFR IgG1 monoclonal antibody (cetuximab) that specifically binds to the extracellular domain of EGFR has been approved by the FDA for clinical use in patients with advanced colorectal cancer and head and neck squamous cell carcinoma [17–19]. In gastric cancers, we previously demonstrated the antitumor efficacy of cetuximab alone and in combination with interleukin 2 (IL-2) as a molecular targeting agent for peritoneal metastasis of EGFR-overexpressing gastric cancers [18]. Therefore, the diagnostic use of this therapeutic antibody to detect gastric cancer peritoneal metastasis has a promising rationale. Another potential diagnostic molecular target is carcinoembryonic antigen (CEA), an established tumor-associated marker for gastrointestinal tract malignancies including gastric cancers. We previously demonstrated that CEA is the most reliable marker for genetic diagnosis of peritoneal wash cytology in gastric cancer patients [20]. Therefore, CEA is another potential target for molecular imaging of peritoneal metastasis of gastric cancers. To date, however, no preclinical study of optical imaging of gastric cancer peritoneal metastasis using NIR fluorophore-labeled EGFR or CEA antibody has been reported.

In the present study, we investigated the sensitivity, specificity, and anatomical accuracy of optical imaging for peritoneal metastasis of gastric cancers using NIR fluorophore-labeled antibody to EGFR or CEA. We further evaluated the usefulness of multimodality imaging combining three-dimensional (3D) fluorescence imaging and MRI. The clinical application possibilities of this multimodality imaging system for gastric cancer peritoneal metastasis are discussed.

Materials and methods

Reagents

Cetuximab and rituximab were purchased from Merck (Darmstadt, Germany) and Zenyaku Kogyo (Tokyo, Japan), respectively. IgG1 human serum was obtained from Sigma-Aldrich (St. Louis, MO, USA). Mouse monoclonal antibody (mAb) to human CEA was purified from supernatant of a hybridoma cell line (HB-8747; ATCC, Manassas, VA, USA) cultured in serum-free medium using a protein G Sepharose column (HiTrap Protein G HP; GE

Healthcare, Uppsala, Sweden). Antibodies used for immunohistochemistry were as follows: mouse monoclonal antibodies for epidermal growth factor receptor (EGFR, PharmDx Kit; DakoCytomation, Glostrup, Denmark), and carcinoembryonic antigen (CEA, clone II-7; DakoCytomation).

Animals

Five- to 6-week-old male athymic nude mice of the KSN strain were purchased from Japan SLC (Hamamatsu, Japan) and maintained under specific pathogen-free (SPF) conditions. Chlorinated water and food autoclaved for 5 min were provided ad libitum. To reduce whole-body, diet-related autofluorescence interference, OpenSource DIET (Research Diet, New Brunswick, NJ, USA or Oriental Yeast, Tokyo, Japan), both nonfluorescent diets, was used. All experiments were carried out with the approval of the Institutional Ethical Committee for Animal Experiments of Aichi Cancer Center Research Institute and met the standard defined by the UK Co-ordinating Committee on Cancer Research guidelines [21].

Cell lines

MKN-28 and GCIY were obtained from RIKEN Cell Bank (Tsukuba, Japan). GLM-1 and GLM-2 were established in our laboratory from surgically resected liver metastases of intestinal-type gastric cancer [22]. These cell lines were maintained in Dulbecco's minimal essential medium (DMEM; Nissui Pharmaceutical, Tokyo, Japan) supplemented with 10 % fetal bovine serum (FBS; Gibco, Grand Island, NY, USA), 100 units/ml penicillin, and 100 μg/ml streptomycin in plastic dishes (BD Falcon; BD Biosciences, Franklin Lakes, NJ, USA) and incubated at 37 °C in 5 % CO_2. The hybridoma cell line (HB-8747) was cultured in serum-free medium (Hybridoma-SFM; Gibco), and supernatant was harvested after 4-day culture.

DNA transfection and isolation of stable luciferase-expressing cells

A firefly luciferase expression vector, pCMV-Luc, was prepared by subcloning a luciferase gene in pTA-Luc vector (Clontech, Mountain View, CA, USA) into pCMV vector containing the neomycin resistance gene (neoR) (Sigma-Aldrich, St. Louis, MO, USA). pCMV-Luc was transfected into MKN-28, GCIY, and GLM-1 cell lines using the FuGENE6 transfection reagent (Roche Diagnostics, Basel, Switzerland). Transfectants were first isolated in selection medium supplemented with 1.0 mg/ml geneticin (G418; Wako, Osaka, Japan). G418-resistant colonies were further screened by limiting dilution in 96-well dishes based on the bioluminescence intensity evaluated with IVIS Lumina II. Resultant cell lines with strong luciferase luminescence, designated as MKN28-Luc, GCIY-Luc, and GLM1-Luc cells, were used in this study.

Immunohistochemistry

Formalin-fixed, paraffin-embedded specimens of peritoneal metastasis from 19 gastric cancer patients and from nude mice after intraperitoneal (i.p.) injection of tumor cells were used in this study. Immunohistochemical staining was carried out with tissue sections 4 μm thick by indirect immunoperoxidase method as described previously [18]. Briefly, the sections were treated with microwave at 98 °C for 10 min. After blocking nonspecific reactions by normal serum for 30 min, these sections were incubated at 4 °C overnight with primary antibodies, thoroughly washed in phosphate-buffered saline (PBS), then incubated with biotinylated secondary antibody. The sections were washed again with PBS and incubated with streptavidin-peroxidase complex (Vectastain ABC kit; Vector Laboratories, Burlingame, CA, USA) for 60 min. The peroxidase-binding sites were visualized using 0.01 % diaminobenzidine (DAB) as the chromogen. Immunostaining of EGFR and CEA was evaluated based on the membrane staining pattern.

Monitoring of peritoneal metastasis with bioluminescence imaging

For monitoring of peritoneal metastasis with bioluminescence imaging, luciferase-tagged tumor cells were harvested with trypsin–EDTA, washed with PBS, and 5×10^6 cells were resuspended in 0.2 ml Hanks balanced salt solution (HBSS) and injected into the peritoneal cavity of nude mice. In 2–3 days or 2–3 weeks after i.p. injection of tumor cells, mice were given i.p. injection with 200 μl D-luciferin (15 mg/ml, ViviGlo Luciferin; Promega, Madison, WI, USA) under 2 % inhaled isoflurane anesthesia, and the bioluminescence images were obtained using the IVIS Lumina II with Living Image software 3.2 according to the manufacturer's protocol (Xenogen, Alameda, CA, USA). For assessment of antitumor activity of cetuximab, mice were divided into a nontreatment control group and a cetuximab treatment group. Cetuximab (1 mg/mouse, twice a week) was given by i.p. injection, starting from day 3 after i.p. injection of tumor cells, for 4 weeks. For assessment of antimetastatic activity of cetuximab, mice were killed after treatment with cetuximab, and the intraperitoneal metastatic nodules were removed and weighed.

In vivo imaging of peritoneal metastasis with fluorophore-labeled cetuximab

For fluorescence in vivo imaging of peritoneal metastasis in nude mice, cetuximab was labeled with XenoLight CF750 using a Fluorescent Rapid Antibody Labeling Kit (Caliper Life Science, Hopkinton, MA, USA) or labeled with indocyanine green (ICG) using ICG-Labeling Kit-NH_2 (Dojindo, Kumamoto, Japan). Mice were injected intravenously (i.v.) (or i.p.) with 0.05 mg XenoLight CF750- or ICG-labeled cetuximab in 250 µl PBS per mouse. After injection, fluorescence imaging of peritoneal metastasis was performed sequentially starting from 10 min to 7 days with IVIS Lumina II using an excitation filter of 745 nm and emission filter of ICG.

3D optical imaging and MRI imaging

To assess the exact localization of metastasis in the peritoneal cavity of mice, three-dimensional (3D) dual bioluminescent and fluorescent imaging of peritoneal metastasis was conducted after i.v. injection of NIR fluorophore-labeled antibody by IVIS Spectrum with Living Image software 4.2 using a mouse imaging shuttle to enhance the fluorescence signal level according to the manufacturer's instruction (Caliper Life Science). After 3D optical imaging, mice were kept under anesthesia by 3,3′-tribromethanol in the mouse shuttle for registration and MRI images were immediately obtained using a Signa 3.0 T clinical scanner equipped with a knee coil (GE Healthcare, Milwaukee, WI, USA) under semisterile condition in a sealed polyethylene bag cleaned with 70 % ethanol.

Three kinds of coronal MRI images were acquired using three standard pulse sequences: 3D spoiled gradient recalled acquisition in the steady state (3DSPGR) for T_1-weighted images, 3D fast spin echo (3DFSE), and fat saturation pulse prepared 3DFSE (FS-3DFSE) for T_2-weighted images. The axial and sagittal images were made by MPR (multiplanar reconstruction) of 3D coronal images. MRI parameters used in this study were as follows: 3DSPGR, repetition time 9.5 ms, echo time 3.3 ms; 3DFSE and FS-3DFSE, repetition time 2,000 ms, echo time 76.7 ms.

Multimodality imaging was reconstructed using 3D optical images and MRI images using the multimodality tool within the same software as Living Image software 4.2 with co-registration between the two images.

Statistics

Student's t test was used to evaluate statistical differences between groups. Significant differences were considered as $p < 0.05$.

Results

Immunohistochemical study of resected specimens of peritoneal metastasis from 19 patients with stage IV gastric cancers revealed that metastatic tumor cells stained positive for EGFR and CEA at an incidence of 79 % (15/19) and 95 % (18/19), respectively (Fig. 1a, b). Based on this high positivity rate, we selected EGFR and CEA as target molecules for optical imaging in this study. Similar immunohistochemical study of xenografted tumors in nude mice showed that MKN28-Luc, GCIY-Luc, and GLM1-Luc cells expressed EGFR strongly (3+), moderately (2+), and weakly (1+), respectively, on the plasma membrane (Fig. 1c). Expression of CEA mRNA evaluated by quantitative reverse transcription-polymerase chain reaction (qRT-PCR) was higher in the following order: GLM-2 > GLM-1 > GCIY > MKN-28 cells (Fig. 1d).

Sequential fluorescence monitoring of peritoneal metastasis of GCIY-Luc cells after i.v. injection of XenoLight CF750-cetuximab (0.05 mg/mouse) demonstrated the pharmacokinetics of XenoLight CF750-labeled cetuximab. The labeled antibody was distributed throughout the body until 1 day post injection and gradually accumulated in the metastatic foci during 1–3 days post injection. Residual unbound antibody was excreted mainly from the kidney, bladder, and liver and washed out from the body until 3–4 days post injection. Labeled antibody was finally restricted to the lesions that almost colocalized to the bioluminescence-positive metastatic foci in the peritoneal cavity until 4–7 days' post injection (Fig. 2a). A similar biodistribution pattern was observed after i.p. injection of XenoLight CF750-cetuximab except for late systemic distribution with several hours of time lag (data not shown). The images continue to be available for at least 4–7 days after injection, irrespective of the injection route, indicating the long-term usefulness of fluorescence imaging with NIR fluorophore-labeled cetuximab compared with bioluminescence imaging.

We examined the specificity of fluorescent imaging for peritoneal metastasis with XenoLight CF750-cetuximab. We found that no significant fluorescent signal was detected in the metastatic foci after i.v. injection of the XenoLight CF750-rituximab, a humanized monoclonal antibody to CD20 (Fig. 2b). In addition, the blocking experiment showed that fluorescence images of peritoneal metastases by MKN28-Luc cells using XenoLight CF750-cetuximab were completely abolished by the co-injection of a tenfold amount of unlabeled cetuximab (data not shown), indicating the specificity of fluorescent imaging using NIR-labeled cetuximab.

ICG is another NIR fluorophore that has been approved for clinical use as a liver function test. Therefore, we next examined the sensitivity and specificity of fluorescent

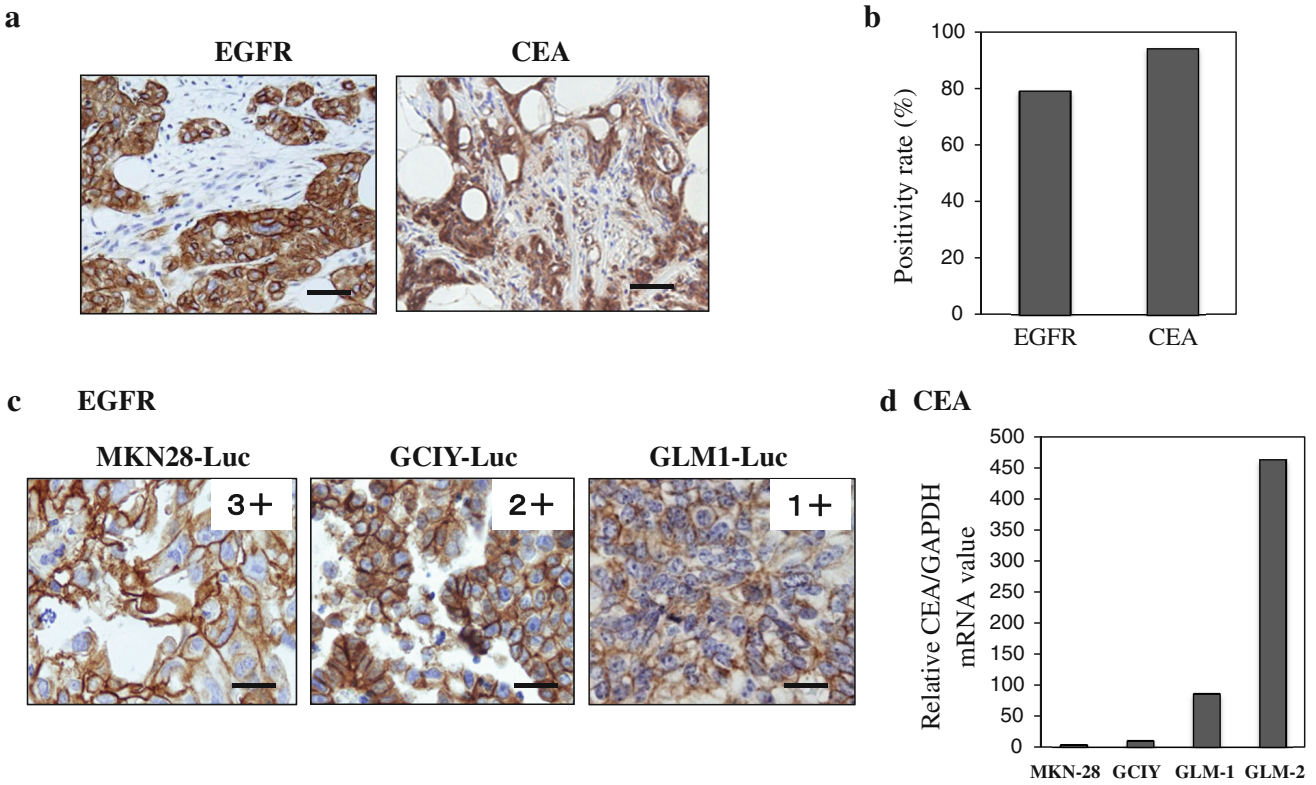

Fig. 1 Epidermal growth factor receptor (*EGFR*) and carcinoembryonic antigen (*CEA*) expression of gastric cancer peritoneal metastasis and gastric cancer cell lines. **a** Immunohistochemistry of formalin-fixed and paraffin-embedded peritoneal metastatic tissues. Note strong membranous and cytoplasmic staining of EGFR and CEA in the tumor cells of the peritoneal metastasis. *Bars* 100 μm. **b** Positivity rate of EGFR and CEA expression of peritoneal metastatic tissues in 19 gastric cancer patients. **c** Immunohistochemistry of subcutaneous tumors in nude mice xenografted with MKN28-Luc, GCIY-Luc, and GLM1-Luc cells. *Bars* 50 μm. **d** Quantitative RT-PCR results for CEA mRNA expression of gastric cancer cell lines

imaging with ICG-labeled cetuximab. Pharmacokinetic analysis showed that ICG-labeled antibody immediately distributed throughout the body and accumulated in the metastatic foci during 1–3 days after i.v. injection. Residual unbound antibody was excreted mainly from the liver and intestine and washed out from the body until 1 day post injection (Fig. 2c). In addition, fluorescent imaging with ICG-labeled human IgG detected no significant signal for peritoneal metastasis (data not shown). Comparative analysis of the fluorescent imaging with XenoLight CF750-cetuximab and ICG-cetuximab revealed that the sensitivity of these fluorescence images was comparable, and both imagings successfully detected not only peritoneal metastasis with high and moderate EGFR expression (MKN-28 and GCIY cells, respectively) at a similar degree but also detected metastasis with low EGFR expression (GLM-1 cell line) (Fig. 2d), indicating similar high sensitivity of fluorescent imaging with ICG-cetuximab to that with XenoLight CF750-cetuximab.

CEA is another target molecule for optical imaging of peritoneal metastasis (Fig. 1). Therefore, we next examined the usefulness of NIR-labeled anti-human CEA mouse MoAb as an imaging probe. Pharmacokinetics of XenoLight CF750-CEA antibody (0.05 mg/mouse) after i.v. injection was essentially the same as that of XenoLight CF750-cetuximab as already described. Pharmacokinetics of ICG-labeled CEA antibody was also similar to that of ICG-labeled cetuximab (data not shown). These NIR-labeled CEA antibodies specifically accumulated in the bioluminescence-positive metastatic foci in the peritoneal cavity in all the cell lines tested depending upon the intensity of CEA expression. In the low CEA-expressing GLM1-Luc cells, fluorescent signals in the metastatic foci were weaker than those in GCIY cells and GLM-2 cells (Fig. 3a, b). Autopsy confirmed that the fluorescence images almost colocalized with luminescence images, which correspond to the metastases in the omentum and mesenterium (Fig. 3b).

Comparative study showed that a macroscopic metastasis measuring 6 × 7 mm in diameter in the omentum could be detected not only by fluorescence imaging with XenoLight CF750-cetruximab but also by MRI (Fig. 4a). On the other hand, a micrometastasis 1–2 mm in diameter could be visualized by optical imaging but not specified by

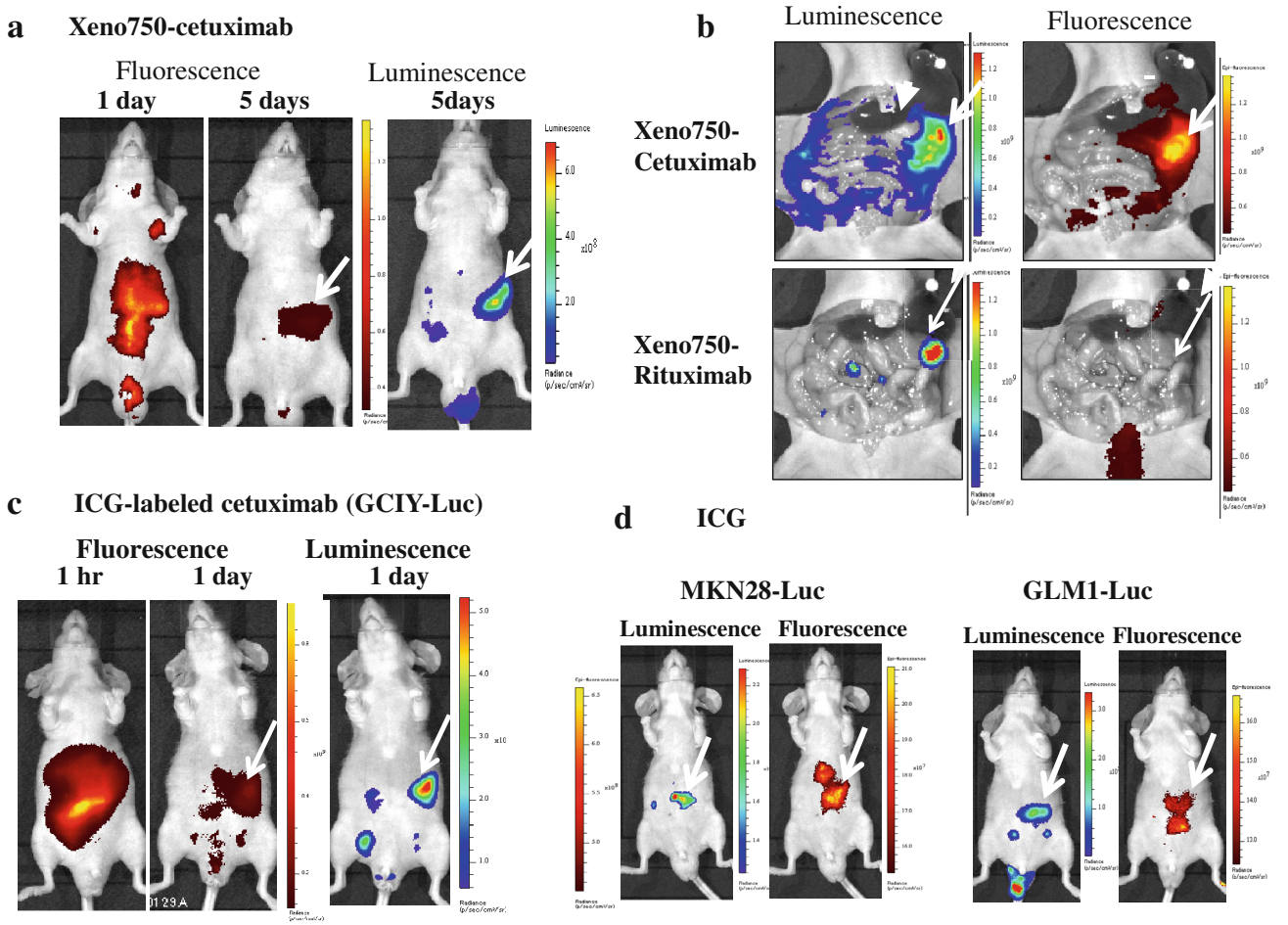

Fig. 2 Pharmacokinetics of XenoLight CF750-cetuximab and indocyanine green (ICG)-cetuximab after i.v. injection into nude mice bearing peritoneal metastasis. **a** Sequential observation of fluorescence images of metastasis (*arrows*) after i.v. injection of xeno750-labeled antibody (50 μg/mouse). Luminescence image (*right*) indicates location of metastasis as a positive control. Note systemic distribution, excretion from kidney/urine, and final accumulation in the peritoneal metastasis. **b** Analysis of specificity of fluorescence imaging for peritoneal metastasis using XenoLight CF750-rituximab as a control antibody. No significant fluorescent signal is seen in the metastatic foci (*arrows*) in the omentum. **c** Sequential observation of fluorescence images of metastasis (*arrows*) after i.v. injection of ICG-labeled antibody (50 μg/mouse). Luminescence image is a positive control. Note systemic distribution, excretion from liver/intestine, and final accumulation in the peritoneal metastasis. **d** Comparison of fluorescence imaging of metastatic foci with high (MKN28-Luc) and low EGFR expression (GLM1-Luc) after i.v. injection of ICG-cetuximab. Note that peritoneal metastasis formed by both cell lines could be successfully detected at a comparable level

MRI with both 3D MIP images and 2D T_2-weighted images (Fig. 4b). These results thereby indicate the higher sensitivity of optical imaging than MRI in micrometastases.

To gain more accurate anatomical localization of the peritoneal metastasis, especially depth information, we developed a 3D bioluminescence and fluorescence imaging method using IVIS Spectrum apparatus with living image version 4.2 software (Fig. 5a). When merged, both luminescence and fluorescence images were almost colocalized in all three directions. Therefore, we next fused optical images with MRI images. The resultant multimodality imaging could successfully specify the anatomical site of peritoneal metastasis in the omentum, which is located below the stomach and right side of the spleen (Fig. 5b). This anatomical diagnosis proved to be accurate in light of autopsy findings (Fig. 5c).

Discussion

In the present study, we developed a new type of multimodality imaging of peritoneal metastasis, combining 3D fluorescence imaging using NIR fluorophore-labeled anti-EGFR or anti-CEA antibody with MRI, for the first time. This whole-body multimodality imaging system has the following advantages. (1) Fluorescence imaging permits sensitive detection of peritoneal micrometastases 1–2 mm

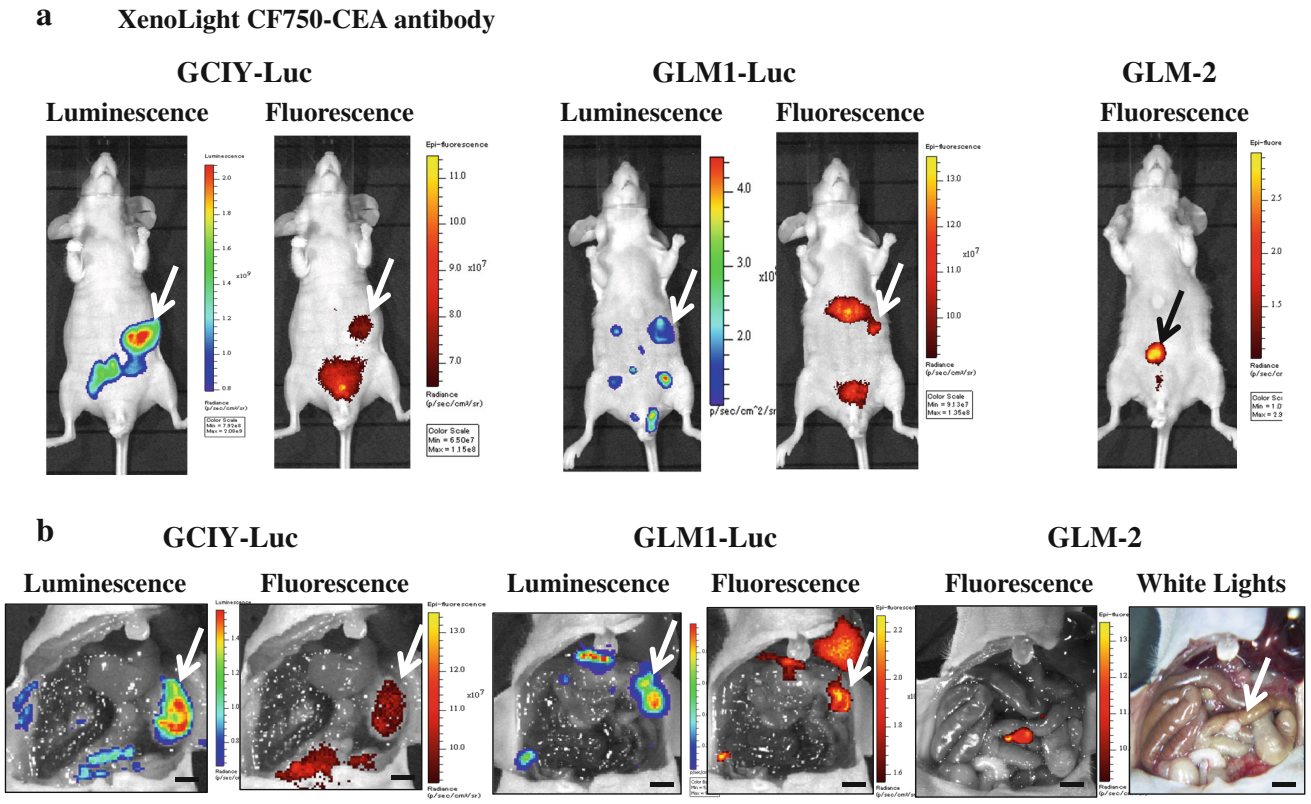

Fig. 3 Fluorescence imaging of peritoneal metastasis formed by gastric cancer cell lines with different CEA expression using XenoLight CF750-CEA antibody. **a** Whole-body fluorescence images of peritoneal metastasis formed by GLM1-Luc, GCIY-Luc, and GLM-2 cells 7 days after i.v. injection of XenoLight CF750-CEA antibody (*right*). Luminescence images are shown as positive controls (*left*). **b** Autopsy images of peritoneal metastasis corresponding to the whole-body images as shown in **a**. Note that most fluorescence images are restricted to metastasis of omentum and mesentery. Metastasis formed by CEA high-expressing GLM-2 cells was clearly visible, but metastasis formed by CEA low-expressing GCIY-Luc cells had weak fluorescence. *Bars* 5 mm

in diameter with sensitivity almost comparable to that of luciferase/luciferin-mediated bioluminescence imaging as a positive control. This fluorescence imaging system can detect peritoneal metastases with relatively low EGFR or CEA expression without need for transfection with reporter genes such as GFP and luciferase. (2) Fluorescence imaging also allows specific detection of EGFR- or CEA-expressing peritoneal metastasis, based on the fact that these images were abolished by excess unlabeled antibody and that NIR-labeled rituximab or human IgG1 did not generate a significant fluorescence signal of the metastatic foci. (3) Multimodality imaging combining optical imaging and MRI allows more accurate diagnosis of the exact anatomical location of the metastasis, which is difficult by 2D or 3D optical imaging alone. (4) ICG-labeled cetuximab, both of which are approved by the FDA for clinical use, shows similar diagnostic sensitivity for peritoneal metastasis to XenoLight CF750-cetuximab, suggesting that optical imaging with this clinically available dye–antibody combination is safe and therefore may have potential for clinical application.

Another interesting finding of this study is the usefulness of EGFR antibody as a molecular probe for diagnostic imaging of peritoneal metastasis in addition to therapeutic utility. In this study, we found that EGFR is overexpressed in the peritoneal metastatic foci at high incidence (79 %) in gastric cancer patients and that cetuximab significantly suppressed growth of peritoneal metastases in an EGFR expression-dependent manner (data not shown). These results provide evidence that EGFR is a promising molecular target for diagnosis of gastric cancer peritoneal metastasis comparable to CEA, which is the established molecular marker for genetic diagnosis of peritoneal washes from gastric cancer patients [20]. To date, there have been several reports on the usefulness of cetuximab for optical imaging [23]. Rosenthal et al. [24] reported the usefulness of Cy5.5-labeled cetuximab for imaging subcutaneous tumor xenografts of head and neck squamous cell carcinoma cell lines in nude mice. However, optical imaging reported previously did not use NIR fluorophore-labeled cetuximab and did not focus attention on whole-body imaging of peritoneal metastases of gastric cancers

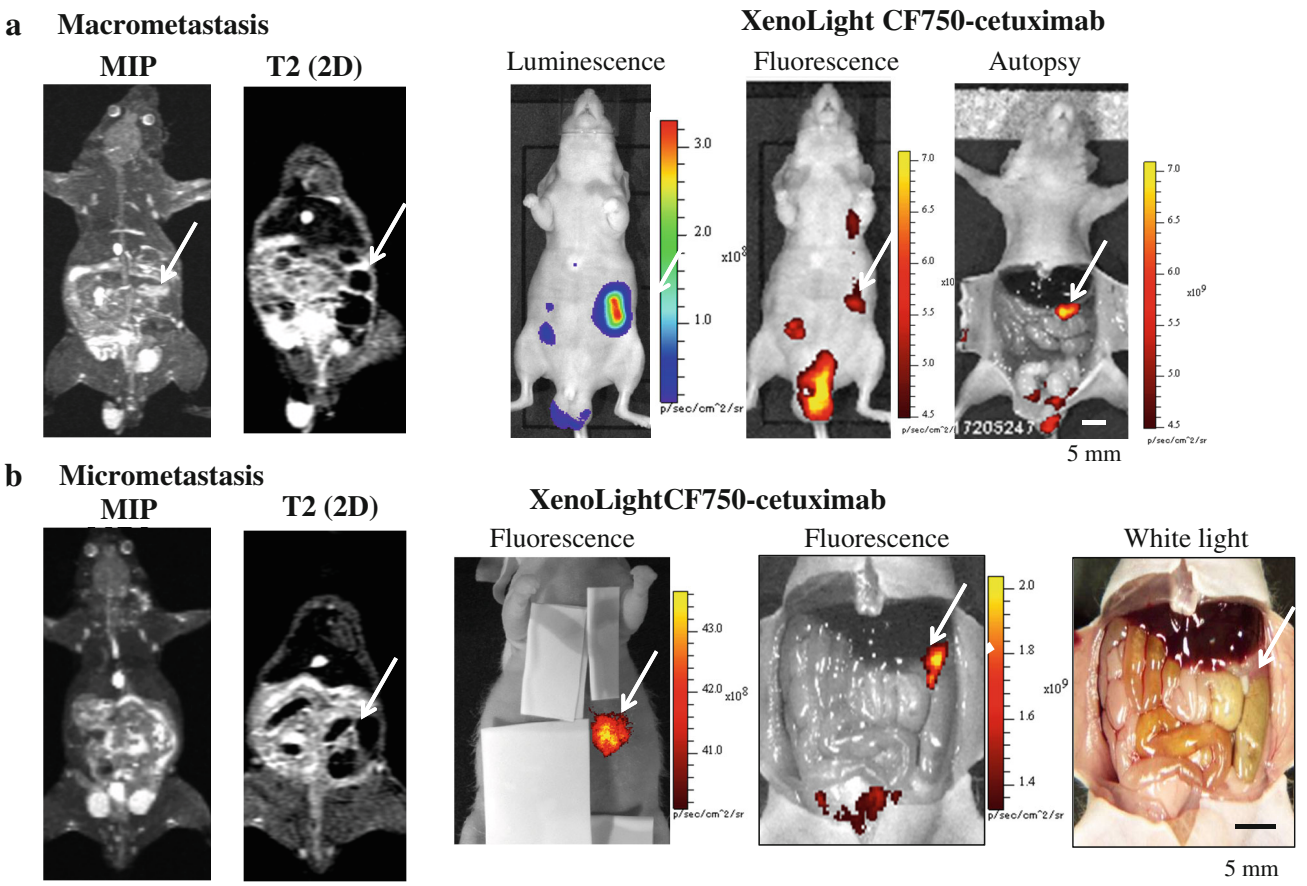

Fig. 4 Comparison of optical and MRI imaging for peritoneal metastasis. **a** MRI (*left*), luminescence (*center*), and fluorescence images (*right*) of macroscopic peritoneal metastasis 6 × 7 mm in diameter. Peritoneal metastasis in the omentum (*arrows*) is detected by MRI and fluorescence imaging using XenoLight CF750-cetuximab. MRI images are represented as 3D MIP (maximum intensity projection) image and 2D fat-suppressed T_2-weighted image. **b** MRI (*left*), fluorescence (*center*), and autopsy images (*right*) of micrometastasis 1–2 mm in diameter. Peritoneal metastasis can be visualized by fluorescence imaging with the aid of a covering sheet to reduce autofluorescence but is unclear by MRI image. MRI images are represented as MIP image and 2D fat-suppressed T_2-weighted image

[25]. Therefore, to our knowledge, this is the first report systematically demonstrating that NIR-labeled EGFR or CEA antibody are good molecular probes for optical imaging of peritoneal metastasis of gastric cancers with EGFR/CEA expression. However, data on the sensitivity and specificity of the present fluorescence imaging were obtained from a mouse xenograft model in combination with chimeric or mouse monoclonal antibody to human EGFR or CEA. In a clinical setting, mesothelial cells and submesothelial stromal cells in the peritoneal cavity of gastric cancer patients may also express EGFR, but not CEA, at a low but significant level, which may result in the generation of some background fluorescence as noise. This potential problem with the clinical use of anti-EGFR antibody as an imaging probe needs to be overcome. However, the background is expected to remain below a significant level, because in the nonmetastatic tissues, distribution of fluorescent-labeled EGFR antibody may be diffuse and not focused to some particular site in the peritoneal cavity.

Preclinical evidence on the usefulness of immune PET imaging using cetuximab labeled with suitable isotopes such as ^{64}Cu, ^{86}Y, and ^{124}I has accumulated [26]. Niu et al. [27] reported that immuno-PET using ^{64}Cu-DOTA-labeled cetuximab enabled visualization and quantification of head and neck squamous cell carcinoma subcutaneous (s.c.) xenografts in nude mice, for example. Advantages of optical imaging with NIR-labeled cetuximab over PET with radiolabeled cetuximab include its convenience and real-time in vivo imaging at lower cost without the genetic risk of ionizing radiation. On the other hand, the major limitation of optical imaging compared with immuno-PET is low depth penetration. In fact, it seems difficult for antibody-mediated fluorescence imaging to detect liver, lung, and bone metastasis at an early stage in mice. However, insofar as peritoneal metastasis in the omentum and mesentery is concerned, which are located in the superficial portion of the abdominal cavity and not covered by hard tissues such as bone or thick muscle layer, the limited tissue penetration of fluorescence imaging can be at

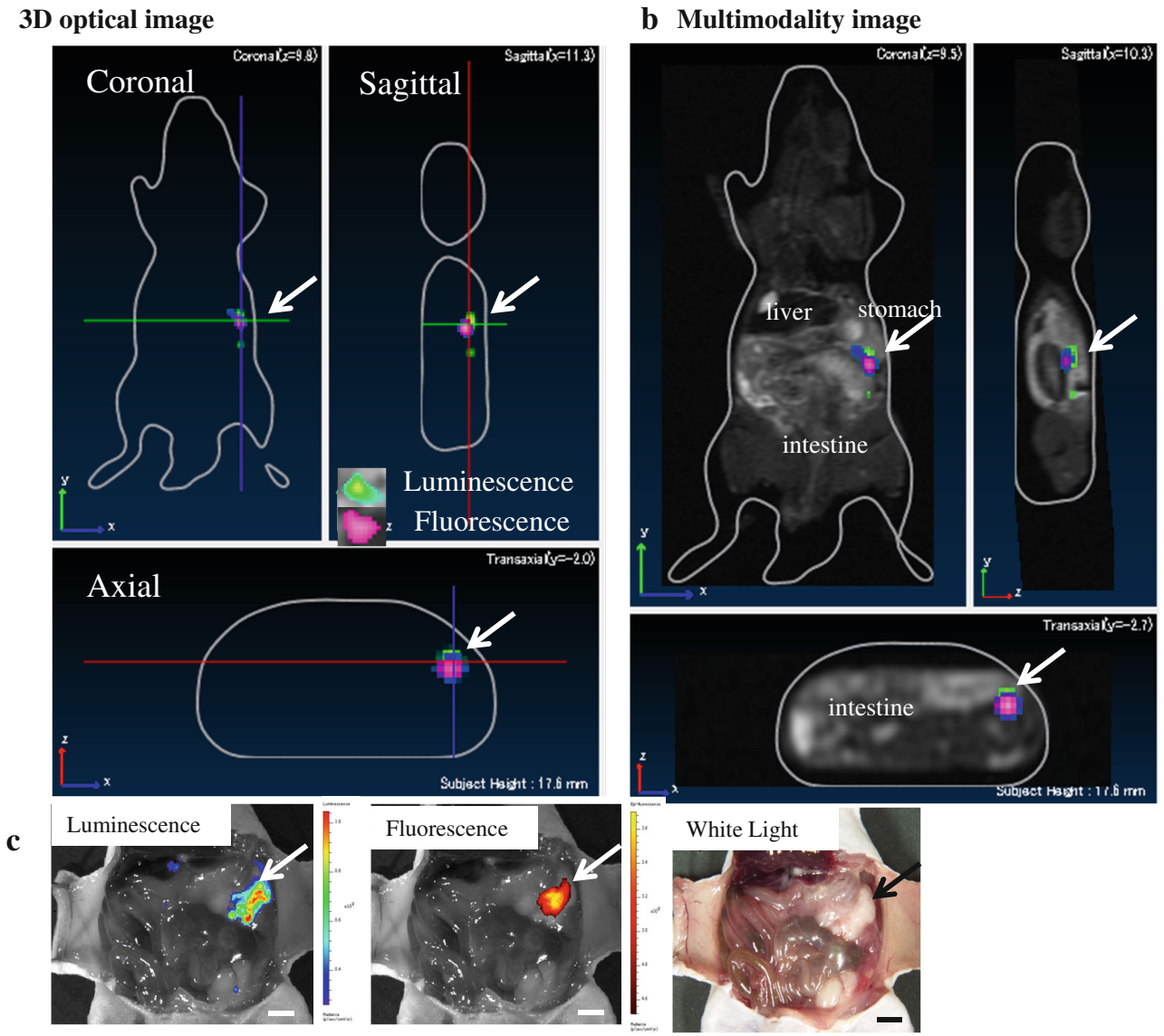

Fig. 5 Multimodality imaging with combination of 3D optical imaging and MRI for peritoneal metastasis. **a** 3D bioluminescence and fluorescence images for metastasis constructed by Ivis spectrum. Colocalization of luminescence image (*green*) and fluorescence image (*red*) for metastasis is clearly seen (*arrows*). **b** Multimodality images constructed by fusion of optical images and MRI image. Anatomical localization of peritoneal metastasis (*arrows*) at the omentum (*below* stomach and *right* side of spleen) is apparent with MRI image. **c** Autopsy finding confirmed the diagnosis by multimodality imaging. *Bars* 5 mm

least partly overcome using NIR-labeled cetuximab. Such fluorescence imaging with NIR-labeled antibodies seems to have clinical significance independent of immuno-PET in the case of peritoneal metastasis.

Optical imaging has the highest sensitivity among all existing modalities, whereas MRI is less sensitive, but provides the highest spatial resolution, the benefit of good anatomical detail, and no exposure to ionizing radiation. In this study, CT was excluded from the choice because of the relatively poor soft tissue contrast without administration of iodinated contrast media to delineate organs and the need for ionizing radiation. Our combination of optical imaging and MRI in this study among many combinations of multimodality imaging results in not only an increase in detection sensitivity but also exact anatomical diagnosis of the location of the peritoneal metastasis. Furthermore, fusion of optical images and MRI images of the same mouse with co-registration was accurately and conveniently done using the mouse imaging shuttle and 3D multimodality tool in the IVIS spectrum system. These results suggest that the present multimodality imaging system has promising potential for accurate and convenient diagnosis of peritoneal metastasis at an early stage and subsequent monitoring of therapeutic response to cetuximab [28].

In conclusion, we developed a new multimodality imaging system combining optical imaging and MRI for peritoneal metastasis in mice and demonstrated that it could visualize gastric cancer peritoneal metastasis at an early stage with high sensitivity, specificity, safety, exact anatomical location, and low cost. Although the sensitivity of fluorescence imaging is still limited to targets that are fairly near the illuminated surface, a brighter NIR light source and more sensitive detection device [29] would offer even more potential for early diagnosis of peritoneal metastasis in gastric cancer patients in future clinical settings.

Acknowledgments We thank Miss K. Nishida for her expert technical assistance. This work was supported in part by a Grant-in-Aid for Scientific Research from the Ministry of Education, Science, Sports, Culture and Technology, Japan and by a Grant-in-Aid for Priority Research Project from Knowledge Hub Aichi, Japan.

Conflict of interest The authors have no conflict of interest.

References

1. Moriguchi S, Maehara Y, Korenaga D, Sugimachi K, Nose Y. Risk factors which predict pattern of recurrence after curative surgery for patients with advanced gastric cancer. Surg Oncol. 1992;1(5):341–6.
2. Sugarbaker PH, Yonemura Y. Clinical pathway for the management of resectable gastric cancer with peritoneal seeding: best palliation with a ray of hope for cure. Oncology. 2000; 58(2):96–107.
3. Kim SJ, Kim HH, Kim YH, Hwang SH, Lee HS, do Park J, et al. Peritoneal metastasis: detection with 16- or 64-detector row CT in patients undergoing surgery for gastric cancer. Radiology. 2009;253(2):407–15.
4. Magota K, Kubo N, Kuge Y, Nishijima K, Zhao S, Tamaki N. Performance characterization of the Inveon preclinical small-animal PET/SPECT/CT system for multimodality imaging. Eur J Nucl Med Mol Imaging. 2011;38(4):742–52.
5. Turlakow A, Yeung HW, Salmon AS, Macapinlac HA, Larson SM. Peritoneal carcinomatosis: role of 18F-FDG PET. J Nucl Med. 2003;44(9):1407–12.
6. Xu H, Eck PK, Baidoo KE, Choyke PL, Brechbiel MW. Toward preparation of antibody-based imaging probe libraries for dual-modality positron emission tomography and fluorescence imaging. Bioorg Med Chem. 2009;17(14):5176–81.
7. Massoud TF, Gambhir SS. Molecular imaging in living subjects: seeing fundamental biological processes in a new light. Genes Dev. 2003;17(5):545–80 (Review).
8. Nakanishi H, Mochizuki Y, Kodera Y, Ito S, Yamamura Y, Ito K, et al. Chemosensitivity of peritoneal micrometastases as evaluated using a green fluorescence protein (GFP)-tagged human gastric cancer cell line. Cancer Sci. 2003;94(1):112–8.
9. Yanagihara K, Takigahira M, Takeshita F, Komatsu T, Nishio K, Hasegawa F, et al. A photon counting technique for quantitatively evaluating progression of peritoneal tumor dissemination. Cancer Res. 2006;66:7532–9.
10. Hoffman RM. Green fluorescent protein imaging of tumour growth, metastasis, and angiogenesis in mouse models. Lancet Oncol. 2002;3(9):546–56.
11. McCann TE, Kosaka N, Turkbey B, Mitsunaga M, Choyke PL, Kobayashi H. Molecular imaging of tumor invasion and metastases: the role of MRI. NMR Biomed. 2011;24(6):561–8.
12. Nolting DD, Gore JC, Pham W. Near-infrared dyes: probe development and applications in optical molecular imaging. Curr Org Synth. 2011;8(4):521–34.
13. Koyama Y, Barrett T, Hama Y, Ravizzini G, Choyke PL, Kobayashi H. In vivo molecular imaging to diagnose and subtype tumors through receptor-targeted optically labeled monoclonal antibodies. Neoplasia. 2007;9:1021–9.
14. Yasumoto K, Yamada T, Kawashima A, Wang W, Li Q, Donev IS, et al. The EGFR ligands amphiregulin and heparin-binding egf-like growth factor promote peritoneal carcinomatosis in CXCR4-expressing gastric cancer. Clin Cancer Res. 2011; 17(11):3619–30.
15. Schlessinger J. Ligand-induced, receptor-mediated dimerization and activation of EGF receptor. Cell. 2002;110:669–72.
16. Tokunaga A, Onda M, Okuda T, Teramoto T, Fujita I, Mizutani T, et al. Clinical significance of epidermal growth factor (EGF), EGF receptor, and c-erbB-2 in human gastric cancer. Cancer (Phila). 1995;75:1418–25.
17. Galizia G, Lieto E, De Vita F, Orditura M, Castellano P, Troiani T, et al. Cetuximab, a chimeric human mouse anti-epidermal growth factor receptor monoclonal antibody, in the treatment of human colorectal cancer. Oncogene. 2007;26:3654–60.
18. Hara M, Nakanishi H, Tsujimura K, Matsui M, Yatabe Y, Manabe T, et al. Interleukin-2 potentiation of cetuximab antitumor activity for epidermal growth factor receptor-overexpressing gastric cancer xenografts through antibody-dependent cellular cytotoxicity. Cancer Sci. 2008;99:1471–8.
19. Pinto C, Di Fabio F, Siena S, Cascinu S, Rojas Llimpe FL, Ceccarelli C, et al. Phase II study of cetuximab in combination with FOLFIRI in patients with untreated advanced gastric or gastroesophageal junction adenocarcinoma (FOLCETUX study). Ann Oncol. 2007;18:510–7.
20. Nakanishi H, Kodera Y, Yamamura Y, Ito S, Kato T, Ezaki T, et al. Rapid quantitative detection of carcinoembryonic antigen-expressing free tumor cells in the peritoneal cavity of gastric cancer patients. Int J Cancer. 2000;89:411–7.
21. United Kingdom Co-Ordinating Committee on Cancer Research (UKCCCR) Guidelines for the Welfare of Animals in Experimental Neoplasia, 2nd edn. Br J Cancer 1998; 77:1–10.
22. Nakanishi H, Yasui K, Ikehara Y, Yokoyama H, Munesue S, Kodera Y, Tatematsu M. Establishment and characterization of three novel human gastric cancer cell lines with differentiated intestinal phenotype derived from liver metastasis. Clin Exp Metastasis. 2005;22:137–47.
23. Barrett T, Koyama Y, Hama Y, Ravizzini G, Shin IS, Jang BS, Paik CH, Urano Y, Choyke PL, Kobayashi H. In vivo diagnosis of epidermal growth factor receptor expression using molecular imaging with a cocktail of optically labeled monoclonal antibodies. Clin Cancer Res. 2007;13:6639–48.
24. Rosenthal EL, Kulbersh BD, King T, Chaudhuri TR, Zinn KR. Use of fluorescent labeled anti-epidermal growth factor receptor antibody to image head and neck squamous cell carcinoma xenografts. Mol Cancer Ther. 2007;6(4):1230–8.
25. Kramer-Marek G, Longmire MR, Choyke PL, Kobayashi H. Recent advances in optical cancer imaging of EGF receptors. Curr Med Chem. 2012;19(28):4759–66.
26. Nayak TK, Regino CA, Wong KJ, Milenic DE, Garmestani K, Baidoo KE, et al. PET imaging of HER1-expressing xenografts in mice with 86Y-CHX-A''-DTPA-cetuximab. Eur J Nucl Med Mol Imaging. 2010;37:1368–76.
27. Niu G, Sun X, Cao Q, Courter D, Koong A, Le QT, et al. Cetuximab-based immunotherapy and radioimmunotherapy of head

and neck squamous cell carcinoma. Clin Cancer Res. 2010; 16:2095–105.
28. Manning HC, Merchant NB, Foutch AC, Virostko JM, Wyatt SK, Shah C, et al. Molecular imaging of therapeutic response to epidermal growth factor receptor blockade in colorectal cancer. Clin Cancer Res. 2008;14:7413–22.
29. Mitsunaga M, Tajiri H, Choyke PL, Kobayashi H. Monoclonal antibody-fluorescent probe conjugates for in vivo target-specific cancer imaging: toward clinical translation. Ther Deliv. 2013; 4(5):523–5.